Dalton Transactions

Accepted Manuscript

This article can be cited before page numbers have been issued, to do this please use: M. Majumdar, R. K. Raut, P. Sahoo and D. Chimnapure, *Dalton Trans.*, 2019, DOI: 10.1039/C9DT00617F.

ROYAL SOCIETY OF CHEMISTRY

rsc.li/dalton

ROYAL SOCIETY OF CHEMISTRY View Article Online
DOI: 10.1039/C9DT00617F

Journal Name

ARTICLE

Versatile coordinating abilities of acyclic N_4 and N_2P_2 ligand frameworks in conjunction with $Sn[N(SiMe_3)_2]_2$

Received 00th January 20xx,
Accepted 00th January 20xx

DOI: 10.1039/x0xx00000x

www.rsc.org/

Ravindra K. Raut [a], Padmini Sahoo [a], Dipti Chimnapure[a] and Moumita Majumdar*[a]

The adaptability of three acyclic tetradentate ligands with –CHR-CHR- (R = H or alkyl substituent) linker in the backbone: bis(α-iminopyridine) **L1** and the reduced form **L2** and diaminodiphosphine **L3** to stabilize various stannylenes have been explored. The reaction of **L1** with two equivalents of $Sn[N(SiMe_3)_2]_2$ led to the stabilization of a bisstannylene **1** through ene-amide transformation of **L1.** Reaction of bisstannylene **1** with $B(C_6F_5)_3$ and silver trifluoromethane sulfonate led to the formation of ligand stabilized Sn(II) dications **2** and **3** respectively. A mixture of Sn(II) dication **3** and a Sn(II) monocation **4** have been obtained from the reaction between **1** and trimethylsilyl trifluoromethane sulfonate. A 1:1 stoichiometric reaction between **L3** and $Sn[N(SiMe_3)_2]_2$ led to the isolation of a dimeric monostannylene **5** having a step-like structure with a Sn_2N_2 central ring. The reaction of **L2** with $Sn[N(SiMe_3)_2]_2$ underwent an electron transfer reaction ultimately leading to bis(α-iminopyridine) isolation.

Introduction

Acyclic tetradentate ligands wherein the two bidentate coordinating fragments are tethered by $–CH_2-CH_2-$ bridges have been widely used in stabilizing a variety of transition metals and lanthanide complexes. The flexibility at the alkyl backbone empowers the ligand denticity to vary from stabilizing mononuclear complexes to bimetallic complexes. Recent examples are the bis(Schiff-base) type ligand bis(α-iminopyridine) crafting bimetallic Cu(I) complexes,[1] polynuclear Fe(III) clusters,[2] dinuclear Ln(III) complexes with single-molecule magnet behaviour,[3] luminescent Zn(II)/Hg(II) complexes,[4] Co(II) coordination polymer[5] etc. Although there are plentiful examples of the utilization of these ligand types in transition metal chemistry, they have been less frequently known in low-valent main group chemistry. With the increasing success of main-group ligand systems in transition metal catalysts and homogeneous catalytic transformations,[6] the stabilization of main-group elements within newer ligand frameworks stands appropriate.

We have successfully explored the potential of such bis(α-iminopyridine) ligand in Group 14 E(II) (E = Ge, Sn) cationic chemistry. The four N donor sites in the bis(α-iminopyridine) **L** (Scheme 1) cumulatively stabilizes a nucleophilic Ge(II) dicationic center as the only example known so far.[7] The torsional amplitude of the $–CH_2-CH_2-$ linker enables the bifunctional modality of the same ligand to stabilize the first

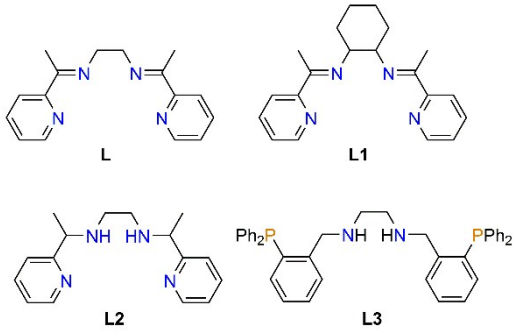

Scheme 1. Ligands **L** and **L1**-**L3**.

bis(chlorogermyliumylidene).[8] Worth mentioning, a bulky bisimino ligand possessing $–CH_2-CH_2-$ backbone has been used to stabilize a boron dication and a dinuclear boron(II) dicationic complex.[9] Furthermore, the ligand **L** being redox-active, underwent reductive cyclization upon reduction of the **L** stabilized bis(chlorogermyliumylidene)[8] and can also be easily reduced to give the bisamine **L2**. The methylimine proton in **L** and **L1** can potentially undergo deprotonation in the presence of a base to generate the ene-amide.[10] Therefore, the versatile binding possibilities make these much coveted ligands (**L**, **L1** and **L2**) to further explore the stabilization of various low-valent main-group compounds.

The tetradentate ligands with a variety of different donor groups N2X2 (X = P, O, S) are intriguing as they potentially impose on the metals to discriminate between binding sites.[11] In recent times, a variety of PNNP tetradentate ligand frameworks have gained popularity in stabilizing pincer-type *N*-

[a] Department of Chemistry, Indian Institute of Science Education and Research, Pune-411008, Maharashtra, India.

† Electronic Supplementary Information (ESI) available: All relevant spectra, crystallographic detail, and DFT calculations. CCDC 1896341 (**1**), 1913314 (**2**), 1913312 (**3**), 1913313 (**4**), 1896344 (**5**). For the ESI and crystallographic data in the CIF or other electronic format see DOI: 10.1039/x0xx00000x

View Article Online
DOI: 10.1039/C9DT00617F

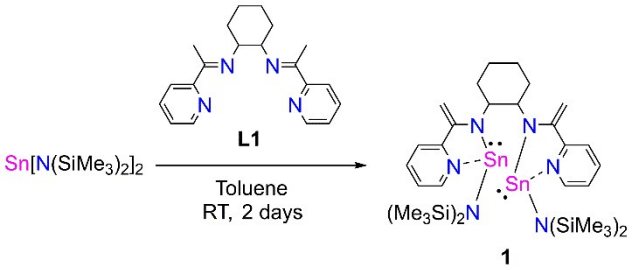

Scheme 2. Syntheses of compound **1**.

Heterocyclic tetrylene (PNNP)E (E = Ge, Sn).[12] Such phosphine functionalized germylene and stannyene pincer-type ligands with a rigid or flexible backbone have emerged as versatile frameworks appropriate for metal coordination and catalytic applications.[13]

Very recently, we have employed the diaminodiphosphine[14] or diiminodiphosphine[15] (PNNP) as bifunctional ligands to host two $[:GeCl]^+$ units, leading to the formation of bis(chlorogermyliumylidene).[16] The steric and electronic effects at the P centre forges the stabilization of the bis(chlorogermyliumylidene) exclusively.[16] Such flexible PNNP ligands have been previously reported to stabilize both dinuclear and mononuclear transition metal complexes as efficient catalysts.[17] Thus, appropriate utilization of this multi-faceted N2P2 ligand in main-group chemistry is certainly a worthwhile study.

In this contribution, we have chosen **L1**-**L3** (Scheme 1) as the three competent ligand frameworks with tetradentate N_4 and N_2P_2 donor sites and studied their coordinating abilities in combination with $Sn[N(SiMe_3)_2]_2$. The facile cleavage of Sn-N bond makes $Sn[N(SiMe_3)_2]_2$ as the appropriate precursor for a variety of stannylene compounds. The formation of a bis(stannylene) by methylimine deprotonation of **L1**, the conversion of **L2** to **L** in the presence of $Sn[N(SiMe_3)_2]_2$, and the formation of dimeric PSnP pincer-type ligand with free P pockets through transamination reaction from **L3** have been discussed. Notably, the hitherto unknown conversion of the bis(stannylene) to a **L1** stabilized Sn(II) dication in the presence of Lewis acids has been reported herewith.

Results and Discussion

Syntheses and Characterizations

Ligand **L1** has been synthesized involving the simple Schiff-base condensation following modified literature procedure.[4] Reduction of **L** using $NaBH_4$ gave **L2**, and reduction of the corresponding diiminodiphosphine with $LiAlH_4$ led to **L3** in acceptable yields (Figures S1-S7, ESI†).

The bisstannylene compound **1** (Scheme 2) was obtained from a reaction between **L1** and $Sn[N(SiMe_3)_2]_2$ taken in a 1:2 ratio in toluene for 2 days at room temperature. Deprotonation of the two methylimines occur to generate the ene-amide stabilized bisstannylene **1** with concomitant elimination of $NH(SiMe_3)_2$ which was removed under reduced pressure. Compound **1** was obtained in 82% yield as an orange precipitate by the addition of small amounts of pentane. Orange coloured single crystals of **1** suitable for X-ray analysis were grown at -40 °C from the hexane solution. Alternately, compound **1** has also been synthesized in good yield of 85% under solvent-free conditions by heating the two precursors **L1** and $Sn[N(SiMe_3)_2]_2$ taken in a 1:2 ratio at 60°C. Notably, very small amounts of metallic tin formation was observed under both the reaction conditions which was removed by filtration from the toluene solution. Compound **1** has been characterized using hetero-nuclear NMR techniques (Figures S8-S11, ESI†). The ^1H NMR spectrum shows the clear disappearance of the $-CH_3$ proton in **L1** and the presence of the terminal H_2C=C protons at 4.87 and 4.43 ppm. The corresponding ^{13}C NMR spectrum shows peak at 82.13 ppm for the terminal alkenyl carbon. A singlet resonance at -47 ppm appears in the $^{119}Sn\{^1H\}$ NMR spectrum of compound **1** in C_6D_6, which falls within the range of reported stannylene chemical shift values.[18,12] UV/Vis spectra of compound **1** in tetrahydrofuran solvent exhibits the longest wavelength absorption λ_{max} = 401 nm (ε = 2797 $M^{-1}cm^{-1}$) (Figures S30-31, ESI†). Worth mentioning, reacting **L1** and $Sn[N(SiMe_3)_2]_2$ in 1:1 ratio also led to the isolation of the bisstannylene **1** as the sole product. There are two literature precedence in main-group chemistry where the redox-active iminopyridine based ligands form ene-amide complexes with Al(III)[19] and Sn(II)[18]. In the case of Sn(II), the 2,6-diiminopyridine ligand (2,6-$[ArN=C(Me)]_2(NC_5H_3)$ (Ar = C_6H_3-2,6-$^iPr_2$)) undergo ene-amide formation only on one side leading to the stabilization of the heteroleptic monostannylene.[18]

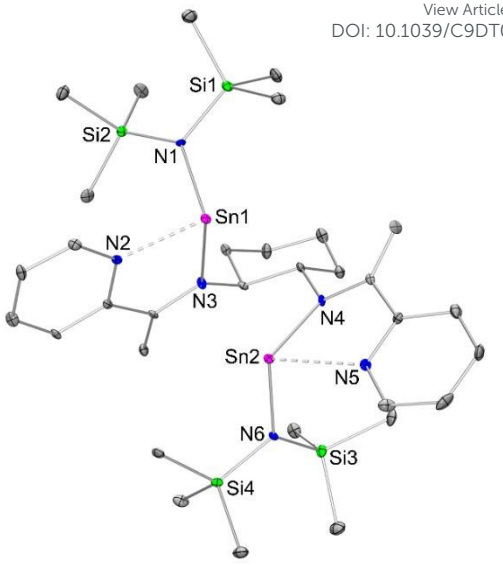

Figure 1. Molecular structure of **1** in the solid state (thermal ellipsoids at 30%, H atoms are omitted for clarity). Selected bond lengths [Å] and angles [°]:Sn1-N1 2.126(5), Sn1-N3 2.191(5), Sn2-N4 2.178(6), Sn2-N6 2.140(5), N2-Sn1-N3 73.1(2), N4-Sn2-N3 71.7(2).

The reactivity of bisstannylene **1** with Lewis acids have been studied. Bisstannylene **1** was reacted with two equivalents of $B(C_6F_5)_3$ at room temperature in toluene to afford the zwitterionic adduct **2** (Scheme 3) with the elimination of one equivalent of $Sn[N(SiMe_3)_2]_2$. The colourless crystals of the zwitterionic **2** was obtained in a yield of 48% by layering with pentane. Compound **2** has been characterized by ^1H, ^{19}F and ^{11}B NMR spectroscopy in $CDCl_3$ (Figures S12-14, ESI†). Two

View Article Online
DOI: 10.1039/C9DT00617F

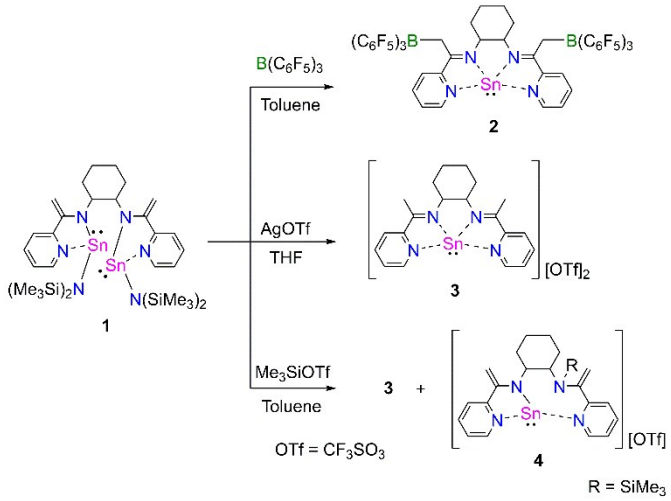

Scheme 3. Reactivity study of compound **1**.

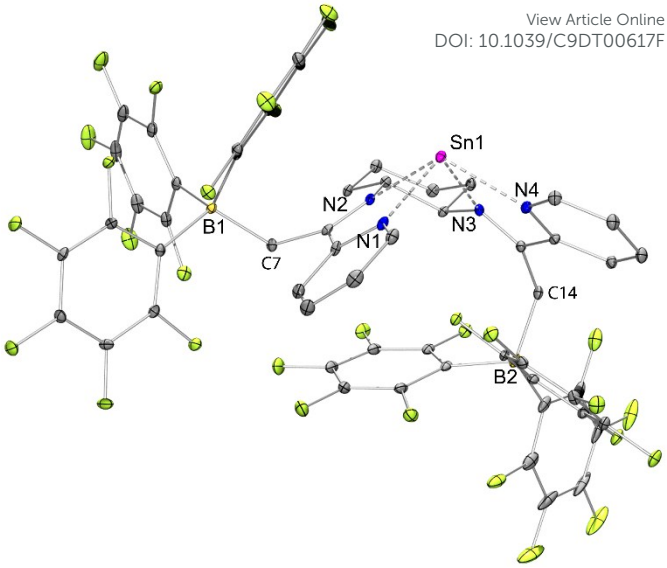

Figure 2. Molecular structure of **2** in the solid state (thermal ellipsoids at 30%, H atoms are omitted for clarity). Selected bond lengths [Å]: Sn1-N1 2.329(3), Sn1-N2 2.274(3), Sn1-N3 2.273(3), Sn1-N4 2.328(3), B1-C7 1.718(5), B2-C14 1.702(5).

peaks at -12.3 and -13.3 ppm appear in the ^{11}B spectrum, revealing the two different environments around the B centers within the molecule even in solution state at the NMR time scale. The ^{19}F NMR spectrum shows peaks that corroborates with the borate group. The characteristic –C*H*$_2$B(C$_6$F$_5$)$_3$ proton peak appears at 3.85 and 3.24 ppm in the ^{1}H NMR spectrum of **2**. ^{119}Sn and ^{13}C NMR were not obtained owing to the poor solubility of the zwitterionic compound **2**. Precedence to zwitterionic adduct formation with B(C$_6$F$_5$)$_3$ have been reported in the case of β-ketiiminate stabilized silylene and germylene.[20] To the best of our knowledge, this is the first example of a stannylene exhibiting such a dipolar behaviour ultimately leading to the conversion to a Sn(II) dication.

The reaction of bisstannylene **1** with silver trifluoromethane sulfonate in tetrahydrofuran at room temperature led to the isolation of crystals of **L1** stabilized Sn(II) dication **3** in 40% yield. Presumably, the solvent acts as the proton source. Compound **3** has been characterized using hetero-nuclear NMR techniques in CD$_3$CN (Figures S15-S18, ESI†). The ^{1}H NMR spectrum of **3** appears considerably downfield shifted compared to the free ligand **L1**, indicating the coordination of the Sn(II) dication to **L1** binding sites. The ^{19}F NMR peak at -79.29 ppm reflects the presence of the triflate anion. The ^{119}Sn NMR spectrum displays a peak at -596 ppm, which is considerably downfield shifted compared to the literature reported chemical shifts of [Sn(C$_7$H$_8$)$_3$][B(C$_6$F$_5$)$_4$]$_2$ (-1468 ppm)[21] and [Sn(CH$_3$CN)$_6$][Al(OR^F)$_4$]$_2$ (R^F = C(CF$_3$)$_3$) (- 1490 ppm)[22] in CD$_3$CN. This suggests that compound **3** has a lower net coordination number in CD$_3$CN. Crystals of stannylene-silver coordination complex[23] has not been obtained from this reaction.

On the other hand, reaction of **1** with two equivalents of trimethylsilyl trifluoromethane sulfonate in toluene at room temperature led to a mixture of products. Layering dichloromethane solution of the reaction mixture with pentane led to co-crystallization of compounds **3** and a Sn(II) monocation **4** in minor amount (Scheme 3 and Figure S19, ESI†). The electrophilic attack of the trimethysilyl cation on the ene-amido nitrogen led to the formation of heteroleptic Sn(II) monocation **4**.

A handful of bisstannylenes have been reported by Hahn et. al. synthesized by a transamination reaction between a tetraamine and Sn[N(SiMe$_3$)$_2$]$_2$.[24] The transamination reaction was revisited in this contribution. In an effort to prepare bisstannylene by transamination, we reacted **L2** with two equivalents of Sn[N(SiMe$_3$)$_2$]$_2$ in tetrahydrofuran at room temperature (Scheme 4). Immediate intense red colouration along with precipitation was observed. Single crystals grown from ethereal solvent post filtration showed the generation of bis(α-iminopyridine) **L** in good amounts (crystallization yield = 70%) after 4 days (Figures S26-S27, ESI†). Essentially, ligand **L2** being redox non-innocent triggers the conversion of the *in situ* generated stannylene to **L** and Sn(0) along with the generation of NH(SiMe$_3$)$_2$. Low temperature ^{119}Sn NMR study in THF-d_8 of the reaction between **L2** and Sn[N(SiMe$_3$)$_2$]$_2$ reveals the initial formation of stannylene via transamination. Subsequently, raising the reaction mixture to room temperature led to the disappearance of the peaks in the ^{119}Sn NMR spectra (Figure

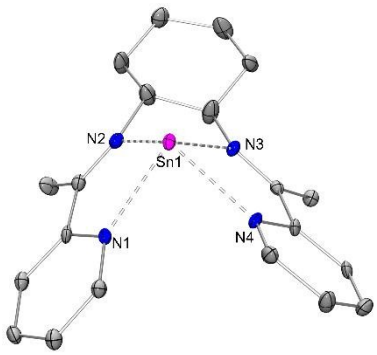

Figure 3. Molecular structure of **3** in the solid state (thermal ellipsoids at 30%, H atoms and triflate counter anions are omitted for clarity). Selected bond lengths [Å]**:** Sn1-N1 2.350(7), Sn1-N2 2.344(8), Sn1-N3 2.301(7), Sn1-N4 2.345(7).

View Article Online
DOI: 10.1039/C9DT00617F

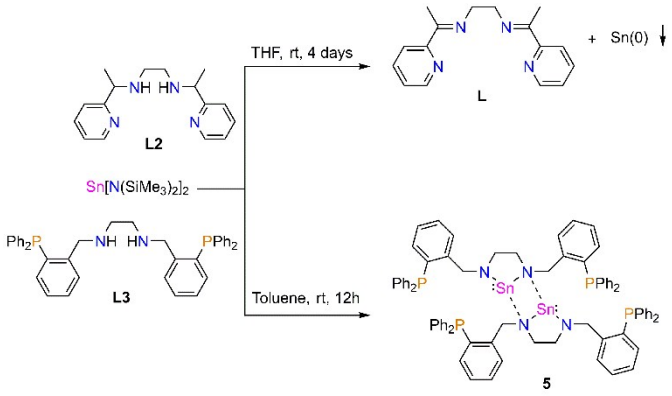

Scheme 4. Transamination reaction between $Sn[N(SiMe_3)_2]_2$ and **L2** and **L3**.

S29, ESI†) due to the formation of metallic tin precipitate. ^{1}H NMR spectrum of the reaction mixture post-workup recorded at room temperature after 4 days shows majorly the formation of L along with small amounts of L2 and stannylene (Figure S28, ESI†). Analogous observation has been reported in the case of a heteroleptic bisstannylene which eventually led to the isolation of 2,6-diiminopyridine stabilized stannylone.[18]

Compound **5** was synthesized by a transamination reaction between **L3** and $Sn[N(SiMe_3)_2]_2$ taken in 1:1 ratio in toluene solvent at room temperature (Scheme 4). Small amounts of metallic tin formed was removed by filtration. Colourless single crystals of **5** appropriate for X-ray diffraction were obtained from the filtrate in good yield of 80%. Compound **5** was characterized in its solution state by NMR spectroscopy in Tol-d_8 (Figures S20-S22, ESI†). Room temperature ^{1}H NMR spectrum in Tol-d_8 shows two broad doublets for the two –CH_2Ar at 4.61 ppm and 4.25 ppm and two peaks for the –CH_2-CH_2- protons at 3.49 ppm and 2.99 ppm corresponding to the dimer **5**. Upon lowering the temperature, these characteristic peaks split further, due to the restricted rotation of the phosphine appendages in the dimer under low temperature conditions (Figure S23, ESI†). The possible free rotations of the phosphine appendages upon rising the temperature causes the peaks to merge as observed in the NMR spectra (Figure S24, ESI†). The further merging of the two peaks each assigned for –CH_2Ar and –CH_2-CH_2- protons provides the diagnostic feature identifying the possible formation of the monomer under high temperature conditions (Figure S24, ESI†). Notably, the NMR peak intensity for the free ligand **L3** increases under higher temperature conditions, hinting the instability of the monomer formed. The ^{31}P{^{1}H} NMR spectrum shows resonances of only one singlet resonance at -15.14 ppm with ^{119}Sn satellites having a weak coupling constant of 165 Hz. Correspondingly a triplet has been observed in the ^{119}Sn{^{1}H} NMR at 46 ppm with a weak Sn···P coupling constant of 173 Hz.[12] Variable temperature ^{31}P{^{1}H} NMR spectra also echoes the phenomenon observed in the proton NMR of **5** (Figure S25, ESI†).

The dimer **5** has been obtained as the only product even when excess of $Sn[N(SiMe_3)_2]_2$ has been taken in the reaction mixture. Worth mentioning, the Sn(II) center in the half unit of **5** has been electronically saturated by the N donor from the other half resulting in a dimeric structure at room temperature. This is unlike the case of phosphine functionalized pincer-type stannylene, where the two P appendages coordinate to the Sn(II) center to stabilize the monomer.[12] Presumably in our case, the presence of the methylene bridge along with the phosphine bulk deters the P → Sn coordination and favours stablilization through dimer **5** formation.

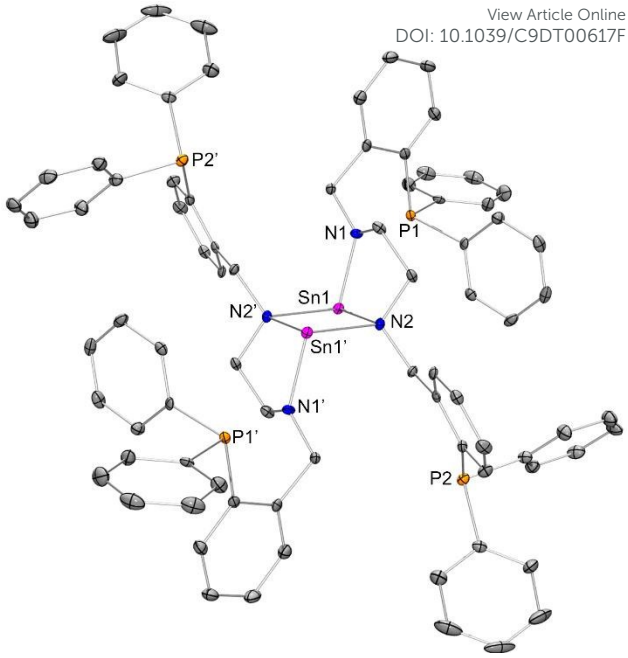

Figure 4. Molecular structure of **5** in the solid state (thermal ellipsoids at 30%, H atoms are omitted for clarity). Selected bond lengths [Å] and angles [°]: Sn1-N1 2.088(3), Sn1-N2 2.235(3), Sn1-N2' 2.299(4), N1-Sn1-N2 80.30(13).

Crystal Structure and Analyses

Compound **1** crystallizes in the monoclinic crystal system with $P2_1/n$ space group (Figure 1 and Table S1, ESI†). The ligand **L1** backbone represents the transformed features with bis(ene-amide) functionality. Each of the two stannylene centers have been stabilized involving two Sn-N covalent bonds of parameters (Å): Sn1-N1 = 2.126(5), Sn1-N3 = 2.191(5), Sn2-N4 = 2.178(6), Sn2-N6 = 2.140(5). The two strong pyridyl N → Sn donor-acceptor bonds of lengths Sn1-N2 = 2.254(6) Å and Sn2-N5 = 2.336(6) Å further stabilize the respective stannylene centers. Both the covalent and coordinate bond parameters in compound **1** agree well with those reported in the literature.[18] While the five-membered ring stabilizing Sn1 is almost planar, Sn2 is raised by 0.72 Å above the N5-C16-C14-N4 coordinating plane. The exocyclic C=C bonds of the five-membered rings stabilizing the two stannylene centers exhibit bond lengths: C6-C7 = 1.352(10) Å and C14-C15 = 1.372(10) Å. Concurrently, the C-N bonds show bond lengths: C6-N3 = 1.386(9) Å and C14-N4 = 1.365(8) Å. The N2-Sn1-N3 and the N4-Sn2-N5 bond angles within the five-membered rings are 73.1(2)° and 71.7(2)° respectively. The two Sn centers are separated by 3.540(8) Å and are canted by a Sn1-N3-N4-Sn2 torsional angle of 90.77(18)° due to the flexible cyclohexyl linker

between the two coordinating fragments. Such bisstannylene geometries serve as appropriate chelating ligands in transition metal chemistry.[24]

Compound **2** crystallized in the monoclinic crystal system with $P2_1/n$ space group as observed in the single crystal X-ray analysis (Figure 2 and Table S2, ESI†). The unit cell shows the presence of three toluene solvent molecules in the crystal lattice. At the core of the molecular structure, the four N donor sites coordinate to the Sn(II) dicationic center with average Sn-N_{im} (im = imino) distance of 2.27 Å and average Sn-N_{py} (py = pyridyl) distance of 2.33 Å. Similar to our earlier reports,[7,25] the four N atoms form a mildly distorted basal coordinating plane (fold angle N3-N2-N1-N4 is approximately 11.65(1)°) with the Sn(II) center being perpendicularly disposed by 1.21 Å. The overall structure appears pyramidal with the sum of bond angle around Sn being 295.7°. This is the second example of a Sn(II) dication after our first report made in early 2019,[25] where the dicationic center is not encapsulated.[26] In the periphery of the molecular structure **2**, the two flanking bulky $B(C_6F_5)_3$ substituents on the methylene carbon are placed at an dihedral angle B1-C7···C14-B2 of approximately 134.8(4)°, with B1···B2 separated by a distance of 7.93(5) Å. The average B-$C_{methylene}$ bond distance is 1.71 Å, indicating that they are single bonds.[20]

The structural formulation of **3** was unequivocally confirmed from single crystal X-ray diffraction studies. Compound **3** crystallized in the triclinic crystal system with P-1 space group (Figure 3, Table S3, ESI†). The structural parameters of **3** are similar to our earlier reported Sn(II) dication.[25] Amongst the four coordinating nitrogen donor sites to the Sn(II) dication center, the two Sn-N_{im} (imino-N atoms) bonds are shorter with bond distances Sn1-N2 2.343(8) Å and Sn1-N3 2.301 (7) Å, while the Sn-N_{py} (pyridyl-N atoms) are slightly longer with Sn1-N1 2.350 (7) Å and Sn1-N4 2.345 (7) Å bond lengths. As in the case of compound **2** and our earlier report,[7,25] the four nitrogen atoms form a slightly distorted basal coordinating plane (fold angle N2-N3-N4-N1 is approximately 13.0(3)°) with the Sn(II) center being displaced perpendicularly by 1.33 Å. The resultant overall dome-shaped or pyramidal structure has a sum of bond angle 285.14° at Sn center. The triflate anion despite it's known weakly coordinating nature, is excluded from the coordination sphere of Sn(II) dicationic center, the closest approach Sn1-O2 distance being 3.014(8) Å.[26] It is apparent from the crystal structures of **2** and **3** that the presence of bulky boryl substituents makes **2** with a comparatively flattened pyramid.

Compound **4** crystallized in the monoclinic crystal system with $P2_1/c$ space group (Figure S31 and Table S4, ESI†). The molecular structure reveals the stabilization of a Sn(II) monocation covalently bonded to the ene-amido nitrogen and electronically saturated by the two pyridyl nitrogens within the unsymmetrical N4 ligand framework (Figure S31, ESI†). The Sn-N_{amido} bond length is 2.095(6) Å and the Sn-N_{py} bond lengths are 2.323(5) Å (Sn1-N1) and 2.311(5) Å (Sn1-N4) bonds. The Sn(II) center is pyramidalised in **4** with the the closest approach Sn1-O1 distance of the triflate anion being 3.080(5) Å.[26]

Compound **5** crystallized in the centrosymmetric P-1 space group as observed in the X-ray analysis (Table S5, ESI†). The solid-state structure shows a dimer of the monostannylene unit (Figure 4). The molecular unit involves a three edge-bridged rings giving rise to a step like structure.[27] The two puckered five-membered diamido-

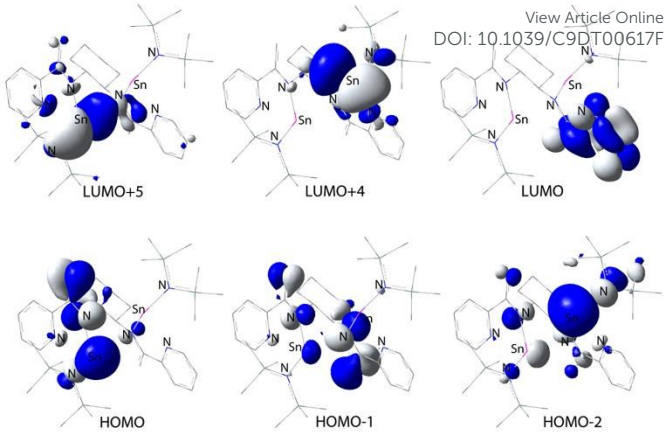

Figure 5. Relevant contour plots of **1'** at an isovalue of 0.04 au.

stannylenes dimerize through N → Sn donor-acceptor interaction to form a central Sn_2N_2 four-membered planar ring. The covalent and coordinate Sn1-N2 and Sn1-N2' bond distances in the central rhomboid are 2.235(3) Å and 2.299(4) Å respectively. The Sn1-N1 covalent bond distance is 2.088(3) Å. Notably, in contrast to N1, N2 acts as a μ_2 bridging donor to the two stannylene centers from the two monomers. Within the four-membered ring the internal N2-Sn1-N2 and Sn1-N2-Sn1 angles are 81.61(14)° and 98.39(14)° respectively. The four pendant phosphine groups in the dimeric structure **5** are away from the stannylene sites, the closest Sn1···P1 distance being 3.785(12) Å. Nonetheless, the presence of flexible methylene in the appendages allow for structural rearrangement and phosphine coordinating sites available for further metallation.[12,13]

DFT Calculations

In order to elucidate the electronic features, DFT calculations were carried out for compounds **1** and **5** at the B3LYP level, using 6-31G(d,p) as the basis set for C, H, N, Si, P and LANL2DZ for Sn.[28] Compounds **1** and **5** have been optimized and the optimized geometries **1'** and **5'** satisfactorily replicates the key metrical parameters (see ESI†). The filled frontier orbitals HOMO to HOMO-2 of **1'** show the maximum contributions from the lone pairs on the two stannylene centers (Figure 5). The LUMO is ligand-centered and reveal the anti-bonding interaction of the terminal C=C (Figure 5). The vacant p-orbital on Sn(II) centers are the energetically high-lying LUMO+4 and LUMO+5 orbitals (Figure 5). The Wiberg bond indices from NBO analysis clearly help to differentiate between the covalent and dative bonds in this molecule. The average WBI values of Sn-$N_{ene-amide}$ and Sn-N_{amide} covalent bonds are 0.35 and 0.45 respectively, while the value for donor-acceptor Sn-N_{py} is comparatively low being 0.23. The average WBI for the C-C bond in the ene-amide is 1.62, reflecting their double bond character. There exists no covalent bonding between the two Sn centers as confirmed from the very low WBI value of 0.18. The Mulliken charges on the stannylene centers are +0.91. The simulated UV/Vis spectrum of **1'** by TD-DFT calculations shows the λ_{max} at 454 nm (HOMO → LUMO+1, *f* =

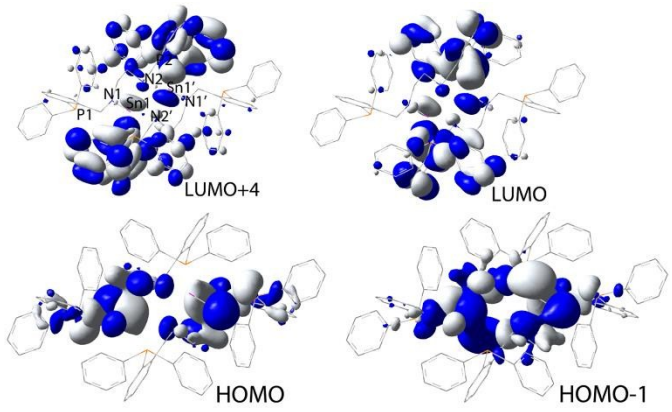

Figure 6. Relevant contour plots of **5'** at an isovalue of 0.02 au.

0.0477), corresponding to the n(Sn) → π^*(L1) transition (see ESI†), which is close by the experimentally obtained value.

The HOMO-1 to HOMO-3 orbitals of **5'** reveal the major contributions from the Sn lone pairs. The vacant p-orbital on the Sn centers are depicted in LUMO along with P-C σ*-π* conjugation and majorly in LUMO+4 (Figure 6). The WBI value for the single bonds N1-Sn1 is 0.48 and N2-Sn1 is 0.32. The difference obviously arises from the bridging donor nature of N2 in contrast to N1 and correlates well with the experimental findings. The Sn1-N2' bond between the two monomeric units in **5'** has a WBI value of 0.29. The dissociation energy of the dimer has been calculated to be 17.3 kcal/mol (see ESI†), implying the favourable dimer formation at room temperature. Furthermore, the dissociation energies have been calculated in toluene, tetrahydrofuran and acetonitrile solvent medium using the polarization continumm model (see ESI†). Although apparently the dissociation energy of the dimer increases with the decrease in dielectric constant of the medium, the change is small (within 0.5 kcal/mol), which indicates that electrostatic interactions do not predominate. Therefore, the formation of the dimer **5** may involve partial covalent interaction.

Conclusions

To summarize, the adaptability of the tetradentate ligands **L1**-**L3** possessing –CH_2-CH_2- backbone linker along with the readily cleavable Sn-N bond in $Sn[N(SiMe_3)_2]_2$ have been utilized to stabilize stannylenes. While **L1** stabilizes a bisstannylene involving ene-amide transformation of the ligand, **L3** stabilizes a monostannylene through the straightforward transamination reaction. However, the monostannylene stabilizes in a dimeric form with four P coordinating sites available for further metallation. The bisstannylene has been observed to undergo the unprecedented conversion to ligand stabilized tin(II) dication by reaction with Lewis acids. The complexation of the bisstannylene and the dimeric monostannylene with transition metals targeting metal clusters for photophysical studies and efficient catalysis are being considered as our current research goals.

Experimental

General Remarks. All manipulations were carried out under a protective atmosphere of argon applying standard Schlenk techniques or in a dry box. Tetrahydrofuran and toluene were refluxed over sodium/benzophenone. Methanol was dried with magnesium cake and stored over 3Å molecular sieves. All the solvents were distilled and stored under argon and degassed before use. Benzene-d_6 and toluene-d_8 were purchased from Sigma Aldrich (Sigma Aldrich Co., St. Louis, MO, USA) and dried over potassium. Acetonitrile-d_3 and tetrahydrofuran-d_8 was purchased from Sigma Aldrich and used as it is. All chemicals were used as purchased. ^{1}H, ^{13}C{^{1}H}, and ^{29}Si{^{1}H} NMR spectra were referenced to external $SiMe_4$ using the residual signals of the deuterated solvent (^{1}H) or the solvent itself (^{13}C). ^{31}P{^{1}H} NMR was referenced to external 85% H_3PO_4. ^{119}Sn NMR was referenced to $SnCl_4$ as the external standard. ^{11}B NMR was referenced to $BF_3.OEt_2$ as the external standard. ^{19}F NMR was referenced to $C_6H_5CF_3$ as the external standard. NMR spectra were recorded on Bruker AVANCE III HD ASCEND 9.4 Tesla/400 MHz and Jeol 9.4 Tesla/400 MHz spectrometer. Solution phase UV/Vis spectra were acquired using a Thermo-Scientific Evolution 300 spectrometer using quartz cells with a path length of 1 cm. Melting points were determined under argon in closed NMR tubes and are uncorrected. Elemental analyses were performed on Elementar vario EL analyzer. Single crystal data were collected on Bruker SMART APEX four-circle diffractometer equipped with a CMOS photon 100 detector (Bruker Systems Inc.) with a Cu Kα radiation (1.5418 Å).

Synthesis of Ligand L1: 6.48 mL (57.7 mmol) of 2-acetyl pyridine was added to solution of 3.47 mL (28.8 mmol) of 1,2-cyclohexyldiamine in 50 mL of dry methanol and reaction mixture was set to reflux for 8 h. MeOH was evaporated from reaction mixture under reduced vacuum. The residue was dissolved in minimum amount of diethyl ether, and flask kept aside to get colourless crystals of ligand **L1** with the yield of 71% (6.56 g). ^{1}H NMR (400 MHz, $CDCl_3$, TMS) δ 8.48 (m, 2H, Pyr-*H*); 7.91 (m, 2H, Pyr-*H*); 7.58 (m, 2H, Pyr-*H*); 7.18 (m, 2H, Pyr-*H*); 3.89 (m, , 2H, -C*H*- Cyclohexyl); 2.35 (s, 6H, -CH_3); 1.94-1.45 (m, 8H, -CH_2-CH_2-cyclohexyl) ppm. ^{13}C{^{1}H} NMR (101 MHz, $CDCl_3$, TMS) δ 164.66 (*C*-CH_3); 158.39(*C*-Pyr); 148.14(*C*-Pyr); 136.31(*C*-Pyr); 123.83(*C*-Pyr); 120.99(*C*-Pyr); 65.70 (-*C*H- Cyclohexyl); 31.58 (-CH_2-CH_2- cyclohexyl); 24.64(-CH_2-CH_2-cyclohexyl); 14.44 (-CH_3) ppm. Elemental Analysis: Calcd. for $C_{20}H_{24}N_4$: C, 74.97; H, 7.55; N, 17.48. Found: C, 75.09; H, 7.63; N, 17.61.

Synthesis of Ligand L2: $NaBH_4$ (0.511 g, 13.51 mmol) was added portionwise in ligand **L** (0.9 g, 3.38mmol) in 20 mL of dry MeOH at room temperature under inert atmosphere. The reaction mixture was stirred for 4h at room temperature. Solvent was evaporated and residue was quenched with water. Product was extracted in dichloromethane, dried over sodium sulphate. Solvent was removed under vacuum yielding 0.81g (90%) pale yellow viscous liquid **L2**. ^{1}H NMR (400 MHz, C_6D_6, TMS) δ 8.42 (td, J = 1.6, 4.8 Hz, 2H, Pyr-*H*); 7.07-7.03 (m, 4H, Pyr-*H*); 6.55 (m, 2H, Pyr-*H*); 3.85-3.77 (m, 2H, -C*H*-CH_3); 2.50-2.43 (m, 4H, -CH_2-CH_2); 1.86 (bs, 2H, -N*H*-); 1.31 (d, J = 8, 6H, -CH_3)ppm. ^{13}C{^{1}H} NMR (101 MHz, C_6D_6, TMS) δ 165.65 (*C*-Pyr); 149.24(*C*-Pyr); 135.69(*C*-Pyr); 121.30(*C*-Pyr); 120.58(*C*-Pyr); 59.68(-H*C*-CH_3); 47.85 (-CH_2-CH_2-); 23.09 (-HC-CH_3) ppm. Elemental Analysis:

Calcd. for $C_{16}H_{22}N_4$: C, 71.08; H, 8.20; N, 20.72. Found: C, 71.25; H, 8.35; N, 20.81.

Synthesis of Ligand L3: Corresponding diiminodiphosphine ligand (1 g, 1.65 mmol) and $LiAlH_4$ (0.282 g, 7.44 mmol) were taken in 30 mL of diethyl ether and stirred at room temperature for 24 hours. The mixture was quenched with water and extracted with DCM. The organic layer was separated and dried over anhydrous Na_2SO_4. The solvent was evaporated under vacuum to obtain a pale yellow sticky solid yielding 0.58 g (57.62%) of **L3**. ^{1}H NMR (400 MHz, $CDCl_3$, TMS) δ 7.45 (ddd, *J*=7 Hz, 4.8Hz, 0.8 Hz, 2H, *H*C-2); 7.34-7.24 (m, 22 H, Ar-*H*); 7.16 (dt, *J* = 7.6 Hz, 0.8 Hz, 2H, *H*C-4); 6.90 (ddd, *J* = 7.6Hz, 4.4Hz, 1.2 Hz, 2H, *H*C-5); 3.92 (s, 4H, Ar-CH_2-NH); 2.50 (s, 4H, -CH_2-CH_2-); 1.55 (br s, 2H, N*H*) ppm. ^{13}C NMR (101 MHz, $CDCl_3$, TMS) δ 144.84(d, *C*-1, $J_{P\text{-}C}$ = 23.81 Hz); 136.94 (d, *C*-6, $J_{P\text{-}C}$=10.15 Hz), 135.81(d, Ar-*C*ipso, $J_{P\text{-}C}$ = 13.75 Hz); 134.06 (d, Ar*C*o, $J_{P\text{-}C}$ = 19.81 Hz); 133.66 (*C*-5); 129.17 (d, Ar-*C*m, $J_{P\text{-}C}$ = 5.48); 129.02 (Ar-*C*p); 128.79 (*C*-3); 128.67 (d, *C*-2, $J_{P\text{-}C}$ = 6.96 Hz); 127.23 (*C*-4); 52.41 (d, N-CH_2, $J_{P\text{-}C}$ = 21.16 Hz); 48.68 (-*C*H_2-*C*H_2-) ppm. ^{31}P NMR (162 MHz, $CDCl_3$, H_3PO_4) δ = -15.42 ppm. Elemental Analysis: Calcd. for $C_{40}H_{38}N_2P_2$: C, 78.93; H, 6.29; N, 4.60. Found: C, 78.91; H, 6.43; N, 4.55.

Synthesis of 1: Method A Toluene (10 mL) was added to a the mixture of ligand L1 (0.4 g, 1.25 mmol) and $Sn[N(SiMe_3)_2]_2$ (1.099 g, 2.5 mmol) and stirred it for 48 h at room temperature. All the volatiles were evaporated under vacuum to get green solid. The green solid was washed with 4-5 mL of pentane to get yellow coloured residue. The yellow residue was further dissolved into diethyl ether and filtered to remove small amount of metallic tin. Solvent was removed under vacuum to get yellow coloured powder 82% (0.87 g) (Decomp. 165 – 167 °C).

Method B Ligand L1 (0.4 g, 1.25 mmol) and $Sn[N(SiMe_3)_2]_2$ (1.09 g, 2.5 mmol) was heated in a schlenk tube at 60°C for 1 h. The residue was washed with small amount of pentane to get orange solid. The solid was dissolved in toluene and filtered to remove small amount of metallic tin. Solvent was removed under vacuum to get orange yellow solid in 85% (0.93 g).

Characterization of **1:** ^{1}H NMR (400 MHz, C_6D_6, TMS) δ 7.66 (ddd, *J* = 5.36, 1.6, 0.84 Hz, 2H, Pyr-*H*); 7.43 (d, *J* = 8.48 Hz, 2H, Pyr-*H*); 6.72 (td, *J* = 7.4, 1.68 Hz, 2H, Pyr-*H*); 6.22 (td, *J* = 0.96, 7.2 Hz, 2H, Pyr-*H*); 4.87 (d, *J* = 1.52 Hz, 2H, C=CH_2); 4.43 (d, *J* = 1.52 Hz, 2H, C=CH_2); 4.15 (d, *J* = 8 Hz, 2H, -C*H*-C*H*- cyclohexyl); 2.97 (d, 2H, *J* = 12 Hz, -C*H*-C*H*- cyclohexyl); 1.83-1.51 (m, 6H, -CH_2-CH_2- cyclohexyl): 0.34 (s, 36H, $SiMe_3$-*H*) ppm. ^{13}C{^{1}H} NMR (101 MHz, C_6D_6, TMS) δ 158.79 (*C*=CH_2); 151.91 (Pyr-*C*); 142.88 (Pyr-*C*); 137.96 (Pyr-*C*); 122.36 (Pyr-*C*); 121.69 (Pyr-*C*); 82.13 C=CH_2); 63.24(-*C*H-*C*H- cyclohexyl); 31.07 (-*C*H_2-*C*H_2- cyclohexyl); 25.71 (-*C*H_2-*C*H_2- cyclohexyl); 6.76 (-Si(*C*H_3) $_3$)ppm. ^{29}Si{^{1}H} NMR (79.53 MHz, C_6D_6) δ -1.30 ppm. ^{119}Sn{^{1}H} NMR (149.74 MHz, C_6D_6) δ -47.05 ppm. Elemental Analysis: Calcd. for $C_{32}H_{58}N_6Si_4Sn_2$: C, 43.84; H, 6.67; N, 9.59. Found: C, 43.89; H, 6.61; N, 9.45.

Synthesis of 2: $B(C_6F_5)_3$ (0.058 g, 0.114 mmol) was added to toluene solution of compound **1** (0.05 g, 0.057 mmol) and the pale yellow reaction mixture was stirred for 1 h at room temperature. The reaction mixture was concentrated and layered with pentane to get colourless crystals of compound **2** with the yield of 48% (0.040 g). Characterization of **2**: ^{1}H NMR (400 MHz, $CDCl_3$, TMS) δ 8.87 (d, *J* = 4.16 Hz, 1H, Pyr-*H*); 8.59 (d, *J* = 5.24 Hz, 1H, Pyr-*H*); 8.27 (d, *J* = 8.08 Hz, 1H, Pyr-*H*); 8.19 (t, *J* = 7.88 Hz, 1H, Pyr-*H*); 7.98 (t, *J* = 8 Hz, 1H, Pyr-*H*); 7.89 (t, *J* = 5.2 Hz, 1H, Pyr-*H*); 7.80 (t, *J* = 6 Hz, 1H, Pyr-*H*); 7.64 (d, *J* = 5.2 Hz, 1H, Pyr-*H*); 3.84 (m, 3H, Cy-*H* & CH_2); 3.57 (t, *J* = 8 Hz, 1H, Cy-*H*); 3.27 (s, 2H, CH_2); 2.57 (d, 2H, Cy-*H*); 1.29 (m, 1H, Cy-*H*); 2.05 (s, 1H, Cy-*H*); 1.95 (d, 1H, Cy-*H*); 1.28 (m, 2H, Cy-*H*): 0.91 (t, *J* = 8 Hz, 2H, Cy-*H*) ppm. ^{19}F{^{1}H} NMR (377 MHz, $CDCl_3$, TFT) δ -164.21 (t, *J* = 19.36 Hz, *m*-F); -163.99 (t, *J* = 19.28 Hz, *m*-F); -159.31 (t, *J* = 20.64 Hz, *p*-F): -159.06 (t, *J* = 20.37 Hz, *p*-F); -129.88 (bs, *o*-F); -130.77 (bs, *o*-F)ppm. ^{11}B{^{1}H} NMR (128.43 MHz, $CDCl_3$, BF_3.OEt_2) δ -13.3 & -12.3 ppm. Elemental Analysis: Calcd. for $C_{56}H_{22}B2F_{30}N_4Sn$: C, 46.03; H, 1.52; N, 3.83. Found: C, 46.50; H, 1.32; N, 3.95.

Synthesis of 3: AgOTf (0.14g, 0.54 mmol) was added to a tetrahydrofuran (20 mL) solution of comp. **1** (0.2g, 0.27 mmol) at room temperature. Colour of the reaction mixture instantly changed from yellow to orange. Reaction mixture was stirred for 1 h at room temperature and then it was concentrated, followed by layering with pentane to get colourless crystals of comp. **3** with crystallization yield of 40% (0.067g).

Characterization of **3**: ^{1}H NMR (400 MHz, CD_3CN, TMS) δ 9.16 (s, 2H, Pyr-*H*); 8.41 (dt, *J* = 8, 1.6 Hz, 2H, Pyr-*H*); 8.31 (td, *J* = 8, 1Hz, 2H, Pyr-*H*); 8.02 (s, Pyr-*H*); 4.56 (s, 2H, Cy-*H*); 2.69 (s, 6H, -CH_3); 2.47 (s, 2H, Cy-*H*); 2.04 (m, 4H, Cy-*H*): 1.66 (t, 2H, Cy-*H*) ppm. ^{13}C{^{1}H} NMR (101 MHz, CD_3CN, TMS) 150.57 (CH_3-*C*); 148.33 (Pyr-*C*o); 143.29 (Pyr- *C*o); 129.41 (Pyr-*C*p); 126.93 (Pyr-*C*m); 125.74 (Pyr-*C*m);122.55, 119.37 (*C*F_3SO_3); 66.64 (Cy-*C*H-); 31.06 (Cy-*C*H_2); 24.61 (Cy-*C*H_2); 17.64 (*C*CH_3) ppm. ^{19}F{^{1}H} NMR (377 MHz, CD_3CN, TFT) δ -79.34 (TMSOTf- *F*) ppm ^{119}Sn{^{1}H} NMR (149.74 MHz, C_6D_6) δ -595.80 ppm Elemental Analysis: Calcd. for $C_{22}H_{24}F_6N_4O_6S_2Sn$: C, 35.84; H, 3.28; N, 7.60. Found: C, 35.98; H, 3.50; N, 7.91.

Reaction of 1 with TMSOTf: Trimethylsilyl trifluoromethane sulphonate (41 µL, 0.228 mmol) was added to toluene solution of compound **1** (0.1 g, 0.114 mmol) and reaction mixture was stirred for 1 h at room temperature. Solvent was removed by evaporation and the residue was dissolved in DCM. Reaction mixture was filtered and filtrate was concentrated. Concentrated DCM solution was layered with pentane to get colourless crystals of compound **3** and **4.**

Synthesis of 5: Toluene (20 mL) was added to mixture of ligand **L3** (0.3g, 0.49 mmol) and $Sn[N(SiMe_3)_2]_2$ (0.22g, 0.49 mmol). The orange reaction mixture was stirred for 12h at room temperature. The pale yellow reaction mixture was filtered and filtrate was concentrated and kept for crystallization to get colourless crystals of compound **5** (Decomp. 128-130 °C) with the yield of 0.28g (80%). ^{1}H NMR (400 MHz, Tol-*d*8, TMS) δ 7.31-7.39 (m, 8H, Ar-*H*); 7.02-7.13 (m, 18H, Ar-*H*); 6.89 (t, *J* = 8 Hz, 2H, Ar-*H*); 4.61 (d, *J*= 16 Hz, 2H, -CH_2Ar); 4.25 (bs, 2H, -CH_2Ar); 3.49 (bs, 2H, -CH_2-); 2.99 (bs, 2H, -CH_2-) ppm. ^{31}P{^{1}H} NMR (162 MHz, Tol-*d*8) δ -16.54 ($J_{p\text{-}Sn}$= 165.55 Hz) ppm ^{119}Sn{^{1}H} NMR (149.27 MHz, Tol-*d*8) δ 46.12 (t, $J_{Sn\text{-}P}$ = 173.20 Hz)ppm

Elemental Analysis: Calcd. for $C_{80}H_{72}N_4P_4Sn_2$: C, 66.23; H, 5.00; N, 3.86. Found: C, 66.19; H, 5.20; N, 3.95.

VT NMR for 5: Compound **5** was dissolved in Tol-d_8 and NMR (^{1}H and ^{31}P) were recorded at temperature ranges from 223 K to 368 K with difference of 20 K.

Deprotonation of L2 by Sn[N(SiMe$_3$)$_2$]$_3$ leading to L: Tetrahydrofuran was added to mixture of ligand **L2** (0.2 g, 0.74 mmol) and Sn[N(SiMe$_3$)$_2$]$_2$ (0.65 g, 1.48 mmol). Immediate colour change with instant precipitate is occurred in the reaction mixture. The reaction mixture was stirred it for 24h at room temperature. Reaction mixture was filtered and solvent was evaporated to get red coloured solid. Solid was dissolved in diethyl ether and kept for crystallization to get 70% (0.14 g) of **L**. ^{1}H NMR (400 MHz, $CDCl_3$, TMS) δ 8.60 (ddd, *J* = 1.2, 2.0, 4.8 Hz, 2H, Pyr-*H*); 8.09 (td, *J* = 0.8, 8 Hz, 2H, Pyr-*H*); 7.71 (td, *J* = 1.6, 7.6 Hz, 2H, Pyr-*H*); 7.29 (ddd, *J* = 1.2, 5.2, 7.2 Hz, 2H, Pyr-*H*); 4.00 (s , 4H, -CH_2 -CH_2 -); 2.45 (s, 6H, -CH_3) ppm. ^{13}C{^{1}H} NMR (101 MHz, $CDCl_3$, TMS) δ 167.60 (*C*-CH_3); 157.82 (Pyr-*C*); 148.33 (Pyr-*C*); 136.37 (Pyr-*C*); 124.11 (Pyr-*C*); 120.98 (Pyr-*C*); 53.62 (-CH_2 -CH_2 -); 14.48 (-*C*H_3)ppm. Elemental Analysis: Calcd. for $C_{16}H_{18}N_4$: C, 72.15; H, 6.81; N, 21.04. Found: C, 72.30; H, 6.95; N, 21.22.

NMR scale reaction: In a NMR tube, THF-*d*8 was added to mixture of ligand **L2** (20 mg, 0.07 mmol) and Sn[N(SiMe$_3$)$_2$]$_2$ (65 mg, 0.14 mmol) at -50°C and shaken well. NMR spectra were recorded at different temperatures.

Conflicts of interest

"There are no conflicts to declare".

Acknowledgements

The authors thank the Department of Science and Technology (DST), India (EMR/2015/001135) and DST Nano-mission Thematic Unit, India (SR/NM/TP-13/2016) for their financial support. The authors thank Dr. Kumar Vanka (NCL Pune, India) for his valuable insights in the computational study.

Notes and references

1 D. E. Díaz, L. Llanos, P. Arce, R. Lorca, J. Guerrero, J. Costamagna, D. Aravena, G. Ferraudi, A. Oliver, A. G. Lappin and L. Lemus, *Chem. Eur. J.*, 2018, **24**, 13839.

2 A. Abhervé, J. M. Clemente-Juan, M. Clemente-León, E. Coronado, J. Boonmark and S. Youngme, *New. J. Chem.*, 2014, **38**, 2105.

3 M. Li, H. Wu, Q. Yang, H. Ke, B. Yin, Q. Shi, W. Wang, Q. Wei, G. Xei and S. Chen, *Chem. Eur. J.*, 2017, **23**, 17775; Q. Sun, P. Chen, H-F. Li, T. Gao, W-B. Sun, G-M. Li and P-F Yan, *CrystEngComm*, 2016, **18**, 4627.

4 X-M. Wang, S. Chen, R-Q. Fan, F-Q. Zhang and Y-L. Yang, *Dalton Trans.*, 2015, **44**, 8107.

5 K. Bhar, S. Khan, J. S. Costa, J. Ribas, O. Roubeau, P. Mitra and B. K. Ghosh, *Angew. Chem. Int. Ed*., 2012, **51**, 2142.

6 W. Wang, S. Inoue, E. Irran and M. Driess, *Angew. Chem. Int. Ed.* 2012, **51**, 3691; A. Brück, D. Gallego, W. Wang, E. Irran, M. Driess and J. F. Hartwig, *Angew. Chem. Int. Ed*. 2012, **51**, 11478; D.Gallego, A. Brück, E. Irran, F. Meier, F. Kaupp and M. Driess, *J. Am. Chem. Soc*. 2013, **135**, 15617; H. Ren, Y. –P. Zhou, Y. Bai, C. Cui and M. Driess, *Chem. Eur. J*. 2017, **23**, 5663; Y. –P. Zhou, M. Karni, S. Yao, Y. Apeloig and M. Driess, *Angew. Chem. Int. Ed*. 2016, **55**, 15096; T. T. Metsänen, D. Gallego, T. Szilvási, M. Driess and M. Oestreich, *Chem. Sci.* 2015, **6**, 7143.

7 R. K. Raut and M. Majumdar, *Chem. Commun.*, 2017, **53**, 1467.

8 M. Majumdar, R. K. Raut, P. Sahoo and V. Kumar, *Chem. Commun*., 2018, **54**, 10839.

9 D. Franz, T. Szilvási, A. Pöthig, F. Deiser and S. Inoue, *Chem. Eur. J.*, 2018, **24**, 4283.

10 B. M. Lindley, P. T. Wolczanski, T. R. Cundari and E. B. Lobkovsky, *Organometallics*, 2015, **34**, 4656.

11 D. Nartop, W. Clegg, R. W. Harrington, R. A. Henderson and C. Y. Wills, *Dalton Trans.*, 2014, *43*, 3372.

12 S. Bestgen, N. H. Rees and J. M. Goicoechea, *Organometallics*, 2018, **37**, 4147; L. Alvarez-Rodriguez, J. Brugos, J. A. Cabeza, P. Garcia-Alvarez, E. Perez-Carreno and D. Polo, *Chem. Commun*. 2017, **53**, 893; J. Brugos, J. A. Cabeza, P. Garcia-Álvarez, E. Pérez-Carreño and D. Polo, *Dalton Trans.*, 2018, **47**, 4534.

13 L. Álvarez-Rodríguez, J. Brugos, J. A. Cabeza, P. García-Álvarez and E. Pérez-Carreno, *Chem. Eur J.* 2017, **23**, 15107; K. M. Krebs, S. Freitag, J. J. Maudrich, H. Schubert, P. Sirsch and L. Wesemann, *Dalton Trans.* 2018, **47**, 83; J. Takaya, K. Miyama, C. Zhu and N. Iwasawa, *Chem. Commun.* 2017, **53**, 3982.

14 R. M. Stoop, S. Bachmann, M. Valentini and A. Mezzetti, *Organometallics,* 2000**, 19**, 4117; C. Sui-Seng, F. N. Haque, A. Hadzovic, A.-M. Pütz, V. Reuss, N. Meyer, A. J. Lough, M. Z. De-Iuliis and R. H. Morris, *Inorg. Chem.,* 2009, **48**, 735.

15 H. Zhang, C. –B. Yang, Y. –Y. Li, Z. –R. Donga, J. –X. Gao, H. Nakamura, K. Murata, T. Ikariya, *Chem. Commun.,* 2003**,** 142; W. Wong, Li Zhang, Y. Chen, W. Wong, W. Wong, F. Xue and T. C. W. Mak, *J. Chem. Soc., Dalton Trans.,* 2000, 1397.

16 P. Sahoo, R. K. Raut, D. Maurya, V. Kumar, P. Rani, M. Majumdar, *Dalton Trans*., DOI: 10.1039/c9dt00109c

17 N. Meyer, A. J. Lough, R.H. Morris, *Chem. Eur. J.,* 2009**, 15**, 5605; C. Sui-Seng, F. Freutel, A. J. Lough, R. H. Morris, *Angew. Chem. Int. Ed*., 2008**, 47***,* 940; J. F. Sonnenberg and R. H. Morris, *ACS Catal.,* 2013, **3***,* 1092.

18 J. Flock, A. Suljanovic, A. Torvisco, W. Schoefberger, B. Gerke, R. Pöttgen, R. C. Fischer and M. Flock, *Chem. Eur. J.*, 2013, **19**, 15504.

19 T. W. Myers and L. A. Berben, *Inorg. Chem.*, 2012, **51**, 1480.

20 M. Driess, S. Yao, M. Brym, C. van Wüllen, *Angew. Chem. Int. Ed.*, 2006, **45**, 6730; A. Jana, I. Objartel, H. W. Roesky, D. Stalke, *Inorg. Chem.*, 2009, **48**, 7645.

21 Schäfer, F. Winter, W. Saak, D. Haase, R. Pöttgen, T. Müller, *Chem. Eur. J*., 2011, **17**, 10979.

22 M. Schleep, C. Hettich, D. Kratzert, H. Scherer, I. Krossing, *Chem. Commun.*, 2017, **53**, 10914.

23 A. E. Ayers, H. V. Rasika Dias, *Inorg. Chem.*, 2002, **41**, 3259.

24 F. E. Hahn, A. V. Zabula, T. Pape, A. Hepp, R. Tonner, R. Haunschild and G. Frenking, *Chem. Eur. J.*, 2008, **14**, 10716; A. V. Zabula, T. Pape, A. Hepp and F. E. Hahn, *Dalton Trans.*, 2008, 5886; A. V. Zabula, T. Pape, A. Hepp and F. E. Hahn, *Organometallics*, 2008, **27**, 2756.

25 R. K. Raut, M. Majumdar, *J. Organomet. Chem.*, 2019, **887**, 18.

26 M. Schleep, C. Hettich, D. Kratzert, H. Scherer, I. Krossing, *Chem. Commun*., 2017, **53**, 10914; J. C. Avery, M. A. Hanson, R. H. Herber, K. J. Bladek, P. A. Rupar, I. Nowik, Y. Huang, K. M. Baines, *Inorg. Chem*., 2012, **51**, 7306; C. L. B. Macdonald, R. Bandyopadhyay, B. F. T. Cooper, W. W. Friedl, A. J. Rossini, R. W. Schurko, S. H. Eichhorn, R. H. Herber, *J. Am. Chem. Soc.*, 2012, **134**, 4332; Schäfer, F. Winter, W. Saak, D. Haase, R. Pöttgen, T. Müller, *Chem. Eur. J.*, 2011, **17**, 10979; A. R. Bandyopadhyay, B.F.T. Cooper, A.J. Rossini, R.W. Schurko, C.L.B. Macdonald, *J. Organomet. Chem.*, 2010, **695**, 1012; T.

View Article Online
DOI: 10.1039/C9DT00617F

Probst, O. Steigelmann, J. Riede and H. Schmidbaur, *Angew. Chem. Int. Ed. Engl.*, 1990, **29**, 1397.
27 S-J. Kim, Y-J. Lee, S. H. Kim, J. Ko, S. Cho and S. O. Kang, *Organometallics*, 2002, **21**, 5358.
28 Gaussian 09, Revision **E.01** Gaussian, Inc., Wallingford CT, 2009.